WILEY

ORIGINAL ARTICLE

Evaluating the Impact of Oceanographic Field Variability on Atlantic Mackerel Distribution Within Russian Fishing Grounds in the Northern Norwegian Sea

M. A. Lebedeva[1,2] | M. V. Budyansky[1,2] | M. Yu. Uleysky[2] | P. A. Fayman[2] | A. A. Didov[1,2] | T. V. Belonenko[1] | D. N. Klochkov[3]

[1]Saint Petersburg State University, Saint Petersburg, Russia | [2]V.I. Il'ichev Pacific Oceological Institute Far Eastern Branch Russian Academy of Sciences, Vladivostok, Russia | [3]MORINFO LLC, Murmansk, Russia

Correspondence: T. V. Belonenko (btvlisab@yandex.ru)

ABSTRACT

Based on fishing records from 2015, 2016, and 2020, this study analyzes the dependence of Atlantic mackerel catch distribution by the Russian fleet on oceanographic conditions in the northern part of the Norwegian Sea (north of 68.5° N). Four types of parameters characterizing fronts and frontal zones are considered: the Lagrangian indicator S, describing water dynamics, along with temperature, salinity, and density in the upper ocean layers, which are traditionally used to identify thermohaline fronts. Gradients of these characteristics are calculated based on these parameters, and the distance from fishing locations to the nearest fronts is evaluated. A unified methodology is applied to automatically define frontal zones using a probability distribution function. To eliminate the dependence of statistical analysis results on limited sampling, a comparison with a random sample was conducted. Histogram analysis of actual catches shows that fishing zones are often located 10–15 km from fronts. It was found that the density of the upper ocean layers has the greatest influence on the distribution of Atlantic mackerel fishing aggregations, while temperature fronts also significantly impact the formation of fishing aggregations.

1 | Introduction

The distribution of forage plankton within mesoscale dynamic structures is of interest not only from a biotic perspective but also in its applications for fisheries, particularly in locating fish aggregations. As the foundation of the food chain, plankton distribution directly impacts the movement and concentration of commercially significant fish species. Studying the environmental conditions that influence the formation of fish aggregations is therefore of particular importance. However, the relationships between fishing grounds in frontal zones and mesoscale eddies, where water masses with significantly different properties converge, leading to both general and localized mixing and the upwelling of nutrient-rich waters, remain underexplored.

Fishing enterprises show significant interest in short-term forecasts of fish aggregation locations, which depend on the dynamics of ocean currents, the positioning of frontal zones, and the distribution of forage resources. Identifying and analyzing these factors can substantially enhance fishing efficiency, promoting more sustainable resource use and optimizing fishing operations. Oceanic fronts, which are boundaries between water masses with different thermohaline properties, create unique conditions that foster plankton and fish aggregations.

These fronts play a critical role in shaping ocean ecosystems by intensifying vertical nutrient exchange, thus boosting biological productivity and ensuring a rich food base for marine organisms. A frontal zone is a region of spatial variability in front location and its temporal evolution. Frontal zones form along the edges of large-scale currents and vary in spatial dimensions, with cross-zonal widths of up to 100 km and depths of up to 1 km. Temporally, they vary from brief events that last only a few hours to enduring structures that remain almost constant. Frontal zones can also develop along the periphery of mesoscale eddies, where vertical movements strongly influence increased biological productivity and the formation of fish aggregations (Owen 1981; Belkin 2021; Prants et al. 2014, 2021; Budyansky et al. 2017).

Species dynamics at higher trophic levels are governed by biological factors—the availability of a food base (plankton and primary production)—and environmental conditions. Drawing on fishing experience and knowledge of the distribution of commercial fish aggregations during feeding migrations, the following hypotheses can be proposed:

1. Fish aggregations develop in convergence zones of currents (positive sea level anomalies) that facilitate the concentration of forage plankton, as well as on the periphery of divergence zones (negative sea level anomalies), where favorable conditions for enhanced productivity across all trophic levels emerge.

2. In stationary convergence zones, such as frontal zones or stationary anticyclonic eddies, plankton may become depleted over time, prompting fish aggregations to relocate to new convergence zones.

3. The most suitable conditions for developing the food base are created by alternating regimes of divergence, which induce the upwelling of nutrient-rich deep waters, thereby promoting the development of lower trophic levels, and convergence regimes, which enhance the concentration of forage plankton. Such conditions are likely to occur in areas with complex seabed topography, including underwater mountains, banks, and topographic slopes (Foux 2009; Owen 1981; Vinogradov et al. 1984; Malinin and Gordeeva 2009).

Ocean frontogenesis remains an understudied phenomenon, as evidenced by the diversity of criteria and ambiguous terminological frameworks used for its description (Fedorov 1983; Gruzinov 1986; Belkin 2002, 2021). Insights into the circulation patterns in this region and the predominant currents are provided in the works of Novoselova, Fayman, et al. (2024) and Volkov et al. (2013, 2015). An oceanic front is a relatively narrow zone characterized by pronounced horizontal gradients of oceanographic properties, such as temperature, salinity, or biogenic element concentrations, which separates larger regions with different vertical structures and stratifications. The evolution of fronts over time and space depends significantly on both external and internal factors (Malinin and Gordeeva 2009). External factors include wind influence, heat exchange with the atmosphere, ocean currents, and tidal processes. Internal factors involve barotropic and baroclinic instability of the flows. The frontal zones of the Norwegian

Sea serve as an example of extensively studied areas, reflected in a large body of literature (e.g., Kostianoy et al. 2004; Kostianoy and Nihoul 2009; Johannessen 1986; Belkin and Cornillon 2007; Smart 1984).

Mesoscale eddies are key dynamic features of the oceanic environment that facilitate the transport and redistribution of water masses, heat, and nutrients. These structures can trap and retain plankton, creating natural "traps" for small marine organisms. The resulting concentration of plankton and other food sources attracts higher trophic levels, including commercially valuable fish species, highlighting the crucial role of mesoscale eddies in supporting fisheries (Vinogradov et al. 1984).

Thus, oceanic fronts and mesoscale eddy structures create areas of high biological productivity in the ocean, where food resources and fish are concentrated, making these regions a priority for fishing. However, at present, there are no reliable statistical estimates of the relationship between the locations of fishing zones and key oceanic parameters. This gap hinders the development of accurate models for predicting fishing zones, which is a critical task for improving the efficiency and sustainability of fisheries.

This study investigates the statistical relationships between the distribution of Atlantic mackerel aggregations, determined post facto by the localization of fishing zones, and the variability of hydrophysical processes, to develop a methodology for statistical forecasting of catches in the Norwegian Sea. Russian vessels fish for Atlantic mackerel, *Scomber scombrus*, primarily in the open part of the Norwegian Sea (OPNS) during the feeding and return migrations from June to October in the upper layers of the water column. Schools are found from the surface down to 30–50 m. As a rule, it inhabits a temperature range of 7.5°C–14°C during the initial feeding period (May–June), and 7.5°C–9°C during return migrations, preferring the higher temperatures within that range. Atlantic mackerel feed on zooplankton (Copepoda, Euphausiidae, Hyperiidae, Appendicularia, Limacinoidea, etc.). Small fish (Myctophidae, Maurolicus) are sometimes found in their stomachs. As a typical plankton feeder, mackerel form dense aggregations in areas of the sea with elevated biomass of food organisms, associated with various oceanographic heterogeneities (Commercial Fish of Russia 2006; Chuksin et al. 1977).

This work aims to create a practical tool for predicting Atlantic mackerel aggregation locations in the Norwegian Sea, addressing a gap in our understanding of their dynamic behavior in this region. Another objective is to identify the set of ecological variables that influence the formation of these aggregations. The identified statistical dependencies may further contribute to a deeper understanding of the dynamics of Atlantic mackerel in response to environmental and physical factors. The primary research methods involve Lagrangian modeling and analysis of frontal zones in both dynamic and thermohaline characteristics. To enhance the broader applicability of these methods, we emphasize the importance of combining multiple oceanographic gradients with fishing ground/catch data within the Lagrangian modeling framework. This integrated approach can make our work valuable not only to specialists focused on specific species or regions but also to a wider range of researchers in oceanography and fisheries science. The study covers the area in the

northern part of the Norwegian Sea (NPNS), where Russian fisheries for Atlantic mackerel are conducted (Figure 1a).

2 | Data

2.1 | Global Ocean Reanalysis GLORYS12V1

For circulation analysis, geostrophic velocities calculated from altimetric data are used, provided by the Copernicus Marine Environment Monitoring Service (CMEMS) at http://marine.copernicus.eu. These data are derived by combining measurements from various altimetric missions covering the period from 1993 to the present. The data fusion process employs the method of optimal interpolation. The spatial resolution of the data is 1/4° in both latitude and longitude and temporally, the data are available with a resolution of 1 day. This approach ensures the creation of a comprehensive and up-to-date dataset, obtained by integrating measurements from different altimetric missions, thereby contributing to a more accurate description of geostrophic velocities in oceanographic studies.

Temperature and salinity data are sourced from the Global Ocean Physics Reanalysis (GLORYS12V1). The GLORYS12V1 product is based on a global real-time forecasting system that uses the Nucleus for European Modelling of the Ocean (NEMO) model and incorporates input data from the European Centre for Medium-Range Weather Forecasts (ECWMF) ERA-Interim. This product integrates both in situ and satellite data from missions such as Topex/Poseidon, Jason-1, 2, Moderate Resolution Imaging Spectroradiometer (MODIS) Terra/Aqua, and Advanced Very High-Resolution Radiometer (AVHRR) from the United States National Oceanic and Atmospheric Administration (NOAA). Satellite-derived sea surface temperature (SST) data were assimilated into the reanalysis. Additionally, it includes ship measurements, data from tide gauges, and drifting buoys, including the Array for Real-time Geostrophic Oceanography (ARGO) data, as well as other in situ observational and oceanographic research data. The integration of observations into the NEMO is achieved through a low-order Kalman filter. GLORYS12V1 accurately captures the complex small-scale dynamics of the ocean surface and demonstrates reliable agreement with independent data not used in the assimilation process. Its reliability makes it a valuable tool for studying various aspects of ocean research and facilitates applications such as short-term forecasting. Spatial averaging of the data was performed at a resolution of 1/12° in both latitude and longitude with a temporal resolution of 1 day.

Because hydrological conditions and the location of thermohaline and dynamic fronts influence the formation of Atlantic mackerel fishing aggregations (Commercial Fish of Russia 2006; Malinin and Gordeeva 2009; Olden and Neff 2001; Owen 1981; Prants 2024; Prants et al. 2014, 2021; Vinogradov et al. 1984), we have utilized these data in our study. We did not use chlorophyll concentration in the analysis because there was persistent high cloud cover in the study area.

2.2 | Fishing Charts

For statistical analysis, fishing data on Atlantic mackerel catches from 2015 (1525 records), 2016 (1521 records), and 2020 (1525 records), provided by the scientific specialists of LLC "MORINFO" (Murmansk), were used.

3 | Methods

3.1 | Lagrangian Modeling

Both traditional statistical methods for oceanographic field analysis and Lagrangian modeling are applied. To implement the Lagrangian method, a large number of artificial (virtual) particles (markers) are placed in the study area on the surface, and then advection equations are solved to track their trajectories:
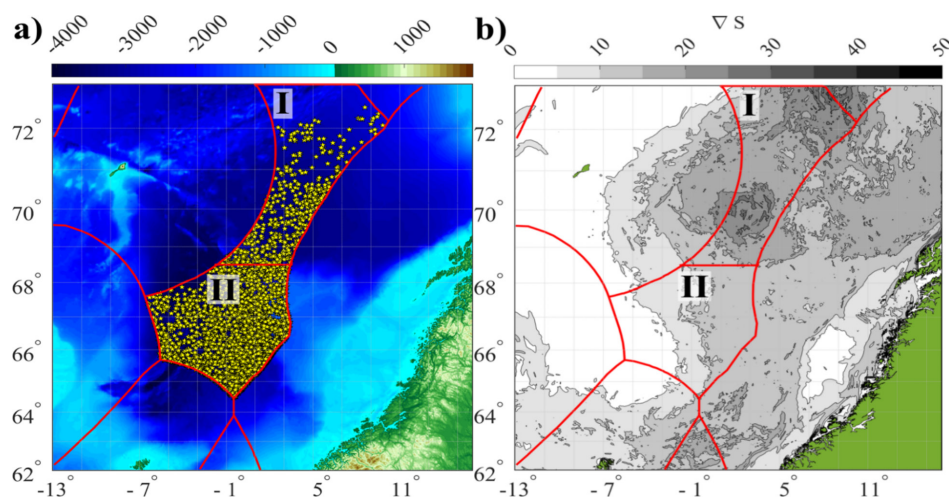

FIGURE 1 | (a) Russian fishing area for Atlantic mackerel in the Norwegian Sea. Red lines indicate the boundaries of specific fishing zones. Stars mark the Atlantic mackerel fishing locations for the 2015, 2016, and 2020 fishing seasons. Bottom topography is shown in color. (b) Spatial distribution of Lagrangian indicator S gradients (km/km). I and II represent the northern and southern parts of the northern part of the Norwegian Sea (NPNS). The spatial distribution of the Lagrangian indicator S gradients is averaged for the 2015, 2016, and 2020 fishing seasons. The x-axis represents longitude in degrees, with negative values indicating west longitude.

$$\frac{d\lambda}{dt} = u(\lambda, \varphi, t), \quad \frac{d\varphi}{dt} = v(\lambda, \varphi, t), \qquad (1)$$

where u and v are the zonal and meridional components of the current velocity, and φ and λ are latitude and longitude in the Mercator coordinate system, respectively. Angular velocities are used because the equations for them have the simplest form on the Earth's sphere. To obtain accurate numerical results, bicubic spatial interpolation and smoothing of the temporal evolution are applied using third-order Lagrange polynomials. Lagrangian trajectories are calculated by integrating Equations (1) using the fourth-order Runge–Kutta scheme with a constant time step of 0.001 days.

The analysis is performed using geographic coordinate mapping of the Lagrangian indicator S characterizing the trajectory length over a given time interval (S-map). The potential of Lagrangian approaches for identifying potential feeding and fishing grounds of pelagic fish and squid is discussed in Prants (2024), which demonstrates that the trajectory length maps (S) contain accumulated information about the "history" of particles moving randomly, including those involved in vortex motion. The length of each tracer's trajectory on the Earth's surface is determined by integrating the advection equations backward in time:

$S = R \int_0^T \sqrt{(\lambda'(t))^2 \cos^2\varphi(t) + (\varphi'(t))^2} \, dt$, where $\varphi'(t)$ and $\lambda'(t)$ are

the time derivatives of latitude $\varphi(t)$ and longitude $\lambda(t)$, and $R = 6371$ km is the Earth's radius. This fundamentally distinguishes from Eulerian characteristics, such as the distribution of oceanographic parameters, which, while containing useful information, are essentially "instantaneous" snapshots of the current moment in time (Novoselova, Travkin, Lebedeva, et al. 2024). Therefore, Lagrangian maps allow a much clearer view of fronts and eddies compared with Eulerian parameter maps (Prants et al. 2013, 2015; Fayman et al. 2019). An additional advantage of Lagrangian approaches is that they allow for the "personalization" of passive tracers, enabling the study of their trajectories over time, thus visualizing their movement in frontal zones and mesoscale eddies.

3.2 | Calculation of Gradients of Eulerian and Lagrangian Characteristics

In the first stage, horizontal gradients of Eulerian and Lagrangian characteristics are calculated at the nodes of a regular grid (i, j) using the following formulas:

$$\frac{\partial C}{\partial x} = \frac{C_{(i,j+1)} - C_{(i,j-1)}}{2S_x}, \quad \frac{\partial C}{\partial y} = \frac{C_{(i+1,j)} - C_{(i-1,j)}}{2S_y},$$

where C is the value of the analyzed parameter at a node of the regular grid, S_x is the grid spacing along the parallel (km), and S_y is the grid spacing along the meridian (km). Due to the convergence of meridians towards the pole, S_x is not a constant value and is calculated using the following formula: $S_x = 1.852 \left| \lambda_{(i,j+1)} - \lambda_{(i,j)} \right| \cos\varphi_{(i,j)}$; S_y is a constant value, which is determined in calculations using the formula:

$S_y = 1.852 \left| \varphi_{(i,j+1)} - \varphi_{(i,j)} \right|$, where 1.852 is the length of one nautical mile in km, and φ and λ are latitude and longitude. The absolute values of the differences $\left| \lambda_{(i,j+1)} - \lambda_{(i,j)} \right|$ и $\left| \varphi_{(i,j+1)} - \varphi_{(i,j)} \right|$ of the values of latitude and longitude were calculated in geographic minutes and converted to kilometers.

The final gradient magnitude of characteristic C is calculated using the formula: $|\nabla C| = \sqrt{\left(\frac{\partial C}{\partial x} \right)^2 + \left(\frac{\partial C}{\partial y} \right)^2}$. This method of calculating gradients has an explicit connection to geographic coordinates (Akhtyamova and Travkin 2023).

For the analysis, horizontal gradients of oceanographic parameters—temperature, salinity, and density (Eulerian characteristics)—as well as the Lagrangian indicator S are calculated. It should be noted that while the calculation of gradients for the spatial distributions of temperature, salinity, or density is a traditional approach commonly used for studying mesoscale fronts, in this study, we additionally employ the Lagrangian indicator S and compute horizontal gradients for this characteristic. The physical meaning of the Lagrangian indicator S is the intensity of mesoscale dynamics. S is measured in kilometers and is determined for each Lagrangian particle as the distance traveled over a specific time interval, which, in our study of synoptic fronts, is taken as 15 days.

3.3 | Fishing Zone Gradient Method (FZGM)

The essence of this method is as follows. Spatial distributions of horizontal gradients of thermohaline (temperature, salinity, water density) and dynamic (Lagrangian indicator S) characteristics are analyzed. For each parameter under consideration, the corresponding distribution functions are constructed. Only those gradient values for which the distribution function exceeds 0.7 (or, more strictly, 0.8) are then considered. The areas where the distribution function values meet these criteria are mapped. In our study, we classify these areas as frontal zones.

The fishery data lack specific spatial resolution and are presented as a set of catch location points. Gradients and distances to these points are calculated independently for each variable, eliminating the need to align their spatial grids. All datasets share the same temporal resolution of 1 day.

Compared with other methods in which frontal zones are also identified based on the gradients of oceanographic parameters, where threshold values are chosen based on certain empirical considerations, the proposed approach determines gradient threshold values automatically. The advantage of this approach, compared with empirical methods, lies in defining gradient thresholds based on rigorous criteria through the analysis of characteristic distributions.

4 | Results

The areas of Russian Atlantic mackerel fishing are located in the Norwegian Sea (Figure 1a). The main fishing activities in

the Norwegian Sea are conducted in two fishing zones: I and II of the OPNS. As seen in Figure 1a, the fishing area I–II is significantly elongated in the meridional direction. In Figure 1b, which shows the map of gradients of the Lagrangian indicator S, it is evident that the fishing area varies greatly in terms of the intensity of dynamic conditions. The S indicator represents the length of the trajectories that Lagrangian particles travel over a specific time interval. The area under consideration was seeded daily with a large number of Lagrangian particles during the fishing periods (June–November) of 2015, 2016, and 2020. The trajectories of these particles were calculated based on the advection Equation (1), with a backward time integration over a given period. The study focused on the rectangular area between 62°–73° N and 13° W–16° E (shown in Figure 1), where 500 × 500 Lagrangian particles were uniformly seeded, and their trajectory lengths in kilometers were calculated for the last 15 days.

In accordance with the research objectives, particular interest lies in the analysis of the gradient the Lagrangian indicator S, which allows for the identification of oceanic fronts, frontal zones, and the boundaries of mesoscale eddies. Because fronts and eddy boundaries are subject to temporal changes in their positions, we averaged the gradient values across all spatial distributions obtained for the study periods. This approach enabled us to delineate the fishing area based on dynamic conditions. The results presented in Figure 1b demonstrate a high degree of dynamic heterogeneity in the Atlantic mackerel fishing area. This indicates the impossibility of a uniform assessment of dynamic conditions and the use of the same parameter gradients across

the entire region simultaneously. For this study, we selected the area I (Figure 1b), located north of 68.5° N. We analyzed the distribution of Atlantic mackerel fishing locations in the context of the gradient distributions of hydro-physical parameters.

In the selected area, a quasi-permanent Lofoten anticyclone is observed (Volkov et al. 2013, 2015; Belonenko et al. 2021; Yu et al. 2017). Areas with elevated values of the Lagrangian indicator S gradient, calculated using the averaging method, indicate a clear association of the Lofoten anticyclone with a specific zone.

Figure 2a,d shows the surface current velocities based on the Archiving, Validation and Interpretation of Satellite Oceanographic (AVISO) data and GLORYS12V1 data for August 2, 2015, as well as the gradients of S and the gradients of thermohaline characteristics on the same date, based on GLORYS12V1 data. The first point to note is that the locations of the frontal zones for the four characteristics considered differ. Let us examine them in more detail. It can be seen that the fishing areas in Figure 2b are located near the maximum values of the S gradients. The points representing the fishing locations are elongated along the isobaths, which characterize the frontal zones—special attention should be given to groups of points near the centers at coordinates 72° N and 10° E, as well as 70° N and 4° E. For temperature (Figure 2e), and particularly for density (Figure 2c), there is a distinct alignment of fishing locations with the frontal zones. This association is less pronounced for salinity, although in the southern part of the studied area, centered at 69° N and
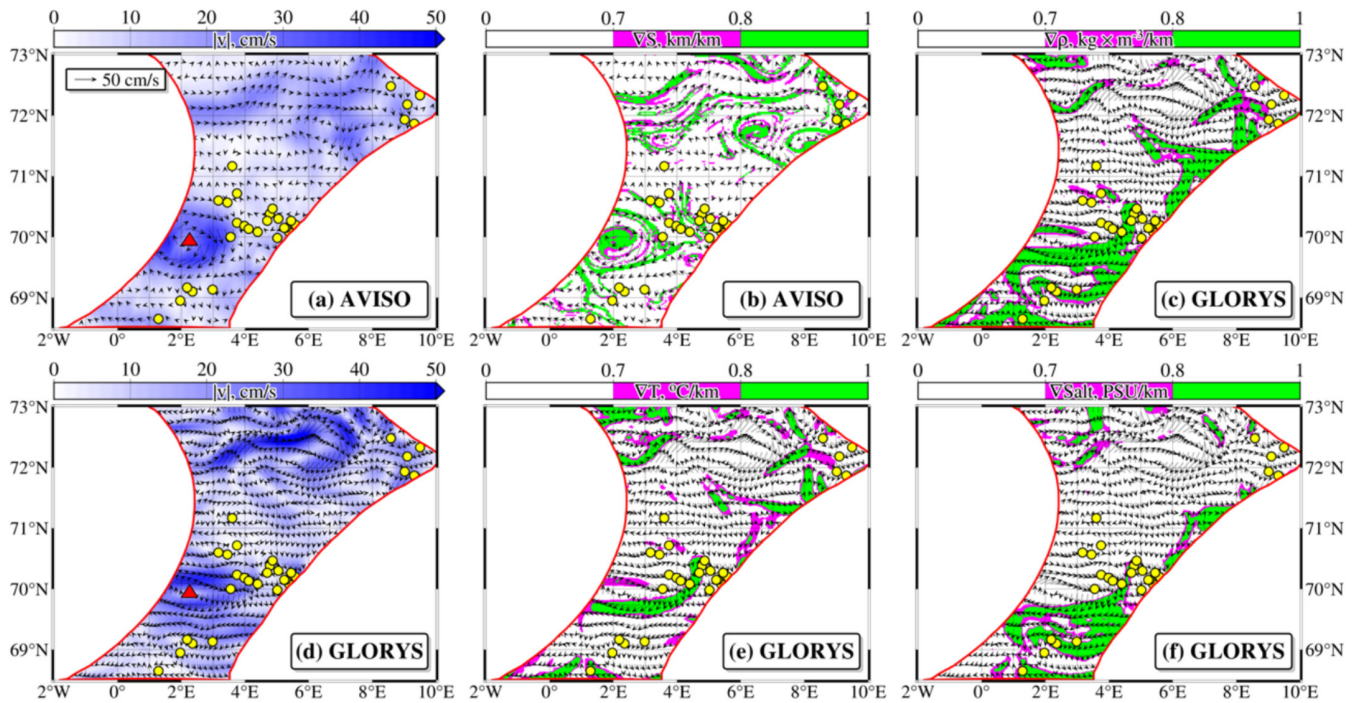

FIGURE 2 | Current velocities in the study area on August 2, 2015 according to the Archiving, Validation and Interpretation of Satellite Oceanographic (AVISO) data (a) and the Global Ocean Physics Reanalysis (GLORYS12V1) data (d); frontal zones in the surface layer: (b) for the Lagrangian indicator S (km), (c) for the density, (e) for the temperature, and (f) for the salinity. Frontal zones where gradient values correspond to distribution function values within the interval [0.7, 0.8] are shown in purple; those corresponding to the interval [0.8, 1.0] are shown in green. Yellow dots indicate fishing locations on August 2, 2015. S is a dynamic parameter; the value of S corresponds to the trajectory lengths, in kilometers, that Lagrangian markers traverse over a defined time interval, which in our study is 15 days. The red triangle indicates the center of the Lofoten anticyclone, based on data from AVISO (a) and GLORYS12V1 (d).

2°E, the group of points representing fishing locations lies directly on the frontal zone (Figure 2f).

To define the criteria for identifying frontal zones and vortex boundaries that separate waters with different characteristics, we calculated the densities and distribution functions of the S indicator gradient values, as well as the distribution of temperature, salinity, and density gradient values for the study area on each date during the fishing period. Here and further, frontal zones in the region are defined as areas where the gradient values correspond to distribution function values of 0.7 and above. For the distribution function values, we consider two intervals: (1) [0.7; 1] and (2) [0.8; 1]. In Figure 2b,c,e,f, the frontal zones are marked in lilac, where the gradient values correspond to the distribution function values in the range [0.7, 0.8], and in green, where the gradient values correspond to distribution function values greater than 0.8. Thus, in our study, the identification of frontal zones for the four characteristics (Figures 2b,c,e,f) follows a unified methodology that eliminates the subjective factor in determining the criteria for identifying frontal zones and is based on the distributions of the values themselves.

For each day of the fishing seasons in 2015, 2016, and 2020, frontal zones were identified in the same manner as shown in Figure 2 for a single date, and then the distances from the fishing locations to the nearest boundary of the corresponding frontal zone were calculated. It should be noted that these distances were determined based on two gradations of the distribution function: with thresholds of 0.7 and 0.8. In other words, these distances were calculated

to the boundary of the lilac or green area, which characterizes the frontal zone (Figures 2b,c,e,f). Statistical analysis was then applied to the obtained estimates. The higher the selected gradient values for defining the frontal zone, the smaller its area (Figure 3). This means that the higher the threshold of the distribution function we choose, the smaller the area of the frontal zone will be.

To eliminate the dependence of the statistical analysis results on the sample size limitation, a comparison with a random sample was performed. For each date within the same period, 1000 random points were generated in the selected area, simulating the fishing locations. A random number generator with a uniform distribution was used to create the random sample. Next, histograms of the distributions of distances from the fishing locations to the nearest gradient of the considered characteristic (S indicator, density, temperature, and salinity) were calculated for each date, both for the actual and the random sample. The histograms were calculated for two thresholds of the distribution function: 0.7 and 0.8. The results are presented in Figures 4 and 5. Analysis of these figures leads to the following conclusions:

1. The analysis of the histograms for the actual catches in Figures 4 and 5 leads to the conclusion that fishing locations are often found not directly on the front but within a 10- to 15-km band near it.

2. Temperature fronts are statistically significant for the formation of fishing concentrations. It can be argued that
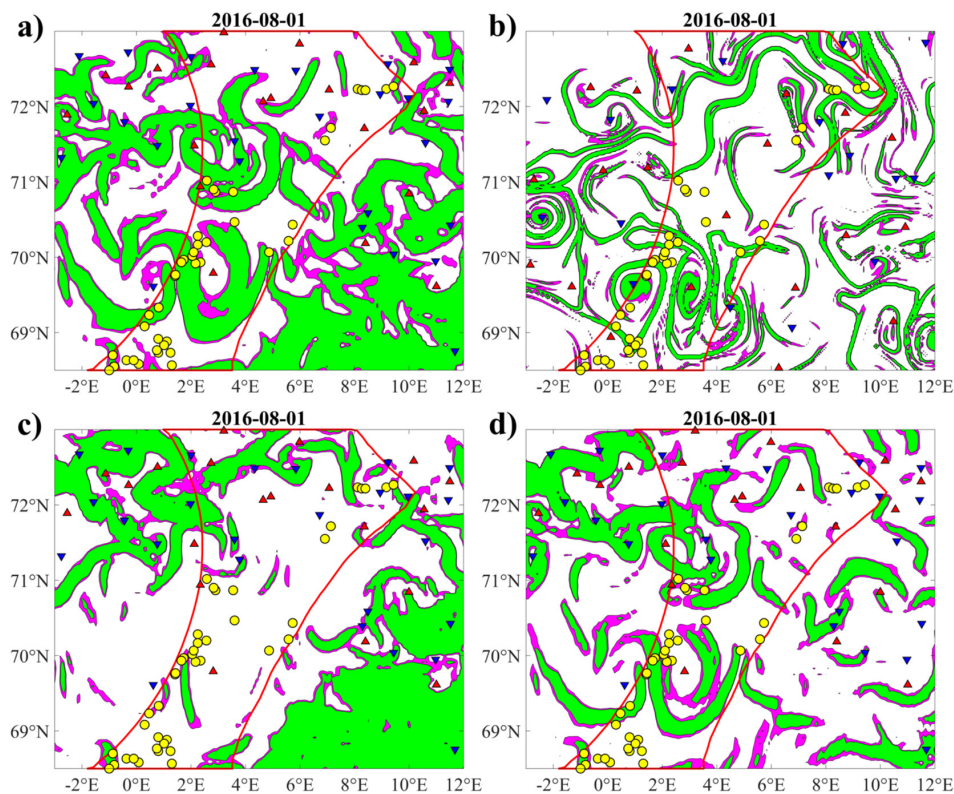

FIGURE 3 | Frontal zones (green and purple), calculated based on the gradients of density (a), the Lagrangian indicator S (b), salinity (c), and temperature (d) for August 1, 2016. Frontal zones where gradient values correspond to the distribution function values within the interval [0.7, 0.8] are shown in purple; those corresponding to the interval [0.8, 1.0] are shown in green. The triangles indicate the centers of the vortices: blue triangles ▼ represent cyclonic vortices, and red triangles ▲ represent anticyclonic vortices.
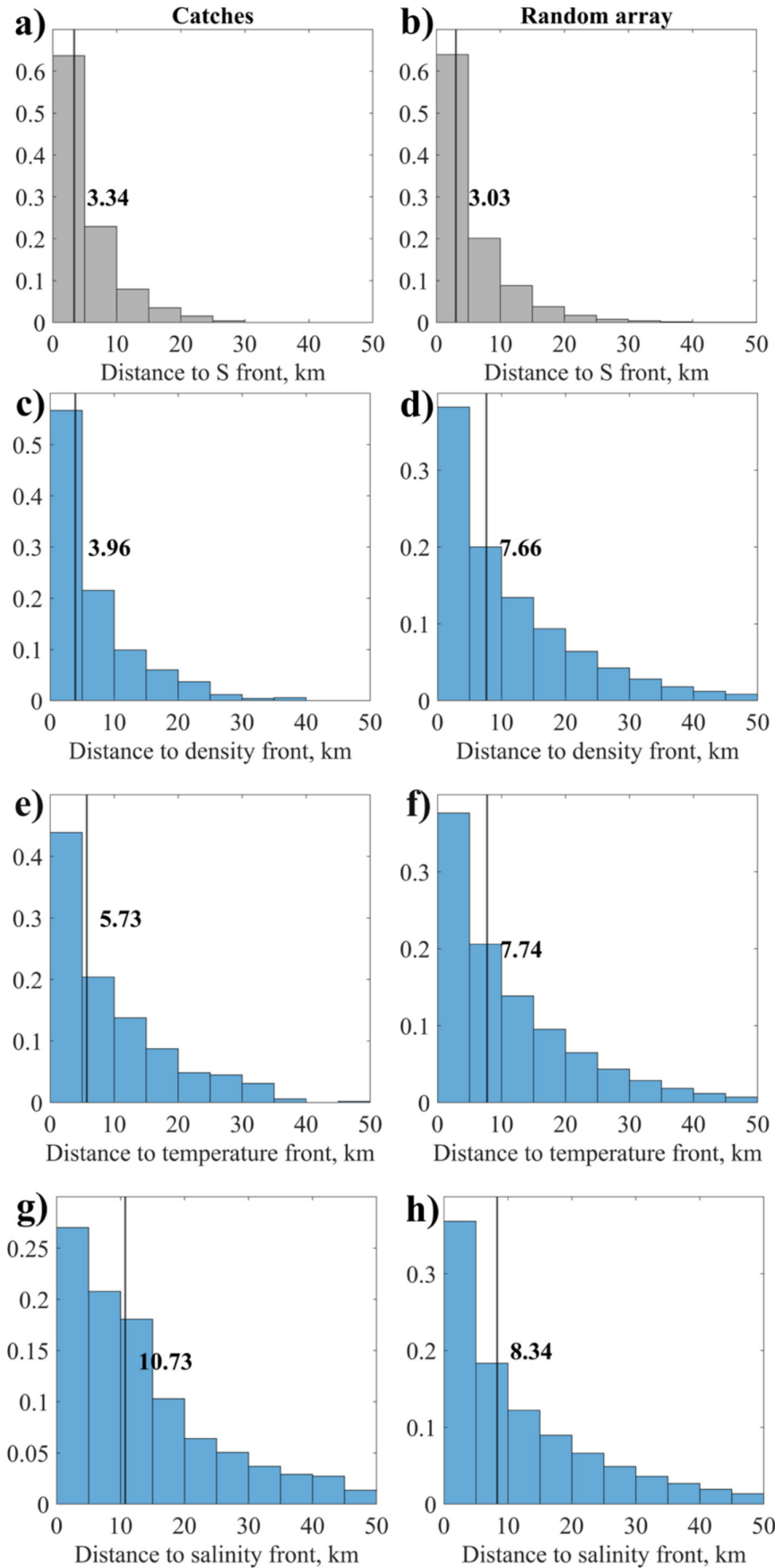
FIGURE 4 | Histograms of distance distributions from fishing locations to the nearest gradient of the Lagrangian indicator S (a, b), density (c, d), temperature (e, f), and salinity (g, h) with a threshold of 0.7, for actual Atlantic mackerel catches in the 2015, 2016, and 2020 fishing seasons (left) and for a random sample on the same dates (right). The black line on the histograms represents the median values for the corresponding sample.

fish, first, avoid areas distant from temperature fronts, as reflected in the smoother distribution in the random sample histogram, and second, are attracted to these fronts, as shown by the shift in the median distribution and the ratio of the heights of the first and second bars when comparing the real catch graphs with the random ones.

3. Although fish do not exhibit similar behavior towards salinity fronts, salinity still influences the formation of concentrations. This is evident in the distributions of distances to density fronts, where fish avoid moving away from them and are more strongly attracted to them than to temperature fronts.

4. In the S histograms, the effect of avoiding areas distant from fronts is quite pronounced, and the effect of the attraction of fishing locations to fronts is more noticeable for the 0.8 thresholds. A different threshold should be considered for the S indicator, as even randomly generated points are very close to the gradients due to the relatively large area with high gradients.

5. In general, when reducing the threshold (i.e., increasing the area of zones with relatively high gradients), the qualitative pattern does not change, but the effects of repulsion/attraction to fronts become less pronounced.

6. The most pronounced effects of avoidance and attraction to fronts are observed for the density gradient. On the graphs, the median distance from the fishing locations to the density gradient is 3.96 km for actual catches, while for the random sample, the median is 7.66 km (for the 0.7 threshold). For the 0.8 threshold, the difference in values is even greater: 5.66 and 12.29 km, respectively. Thus, density is the most representative characteristic when determining the influence of hydrodynamic and thermohaline conditions on fishing activity.

5 | Discussion and Conclusions

This study proposes a methodology for identifying frontal zones based on statistical estimates. Four types of parameters characterizing fronts and frontal zones in the fishing area are considered: the Lagrangian indicator S, describing the dynamics of water, as well as temperature, salinity, and density, which are traditionally used to identify thermohaline fronts (Commercial Fish of Russia 2006; Malinin and Gordeeva 2009; Olden and Neff 2001; Owen 1981; Prants 2024; Prants et al. 2014, 2021; Vinogradov et al. 1984). Gradients of these characteristics are calculated for each parameter.

The statistical analysis is performed not on the characteristics themselves but on their gradients. Frontal zones are determined from the gradient values, for which probability distribution functions are constructed. Two cutoff values of the function are then selected for probabilities greater than 0.7 and 0.8. In this way, the subjective element, in which the researcher assigns a specific gradient value that they believe characterizes a front, is eliminated. In our approach, such a criterion is chosen based on the distribution function values and is uniformly applied to all four parameters.

Based on the distribution functions with cutoff values > 0.7 and > 0.8, two types of frontal zones are identified. The next step involves calculating the distances from the actual fishing locations to the nearest fronts for each of the four parameters, for which distribution histograms are constructed based on the distance in kilometers. For comparison, the same procedure is carried out for a random sample of 1000 points, simulating fishing locations.

This approach helps identify potential patterns and relationships between fishing locations and factors influencing the catch. The constructed distribution histograms clearly illustrate how the distance to the nearest fronts correlates with the selected parameters, revealing both positive and negative correlations. Additionally, the analysis of the random sample serves as a control group, allowing an assessment of how the real data deviates from the theoretically expected values.

Our data show that density has the strongest influence on the distribution of Atlantic mackerel fishing aggregations. It is worth noting that in the study by Vinogradov et al. (1984), which analyzes the biological productivity of dynamically active zones of the open ocean, including the North Atlantic region, it is indicated that areas with high-density gradients often coincide with known fishing grounds. This is also supported by expeditionary fishing research in the region. Our research, conducted using statistical analysis, confirms this result.

The analysis of the histograms of actual catches shows that Atlantic mackerel fishing zones are often located 10–15 km from the fronts. In our study, it was found that temperature fronts have a significant impact on Atlantic mackerel concentration: fish tend to avoid areas far from the fronts, as seen in the smooth distribution of the random sample, and are attracted to them, as evidenced by the shift in the medians of the distributions and the difference in the heights of the bars for the real and random data. Although fish do not exhibit similar behavior concerning salinity fronts, salinity still affects concentration, as shown by the fish's tendency towards density fronts. On the S-histograms, the effect of avoiding areas distant from fronts is more clearly expressed with a cutoff of 0.8, but the high density of gradients requires adjustment. When the cutoff is reduced, i.e., when the zones with high gradients are expanded, the effect of avoidance and attraction to fronts becomes less pronounced, although the overall picture remains unchanged.

Author Contributions

Lebedeva M.A.: investigation, visualization. **Budyansky M.V.:** software, formal analysis, data curation, supervision, investigation. **Uleysky M.Yu.:** resources, investigation, methodology. **Fayman P.A.:** software, validation. **Didov A.A.:** software, visualization. **Belonenko T.V.:** project administration, funding acquisition, formal analysis, writing – review and editing. **Klochkov D.N.:** resources.
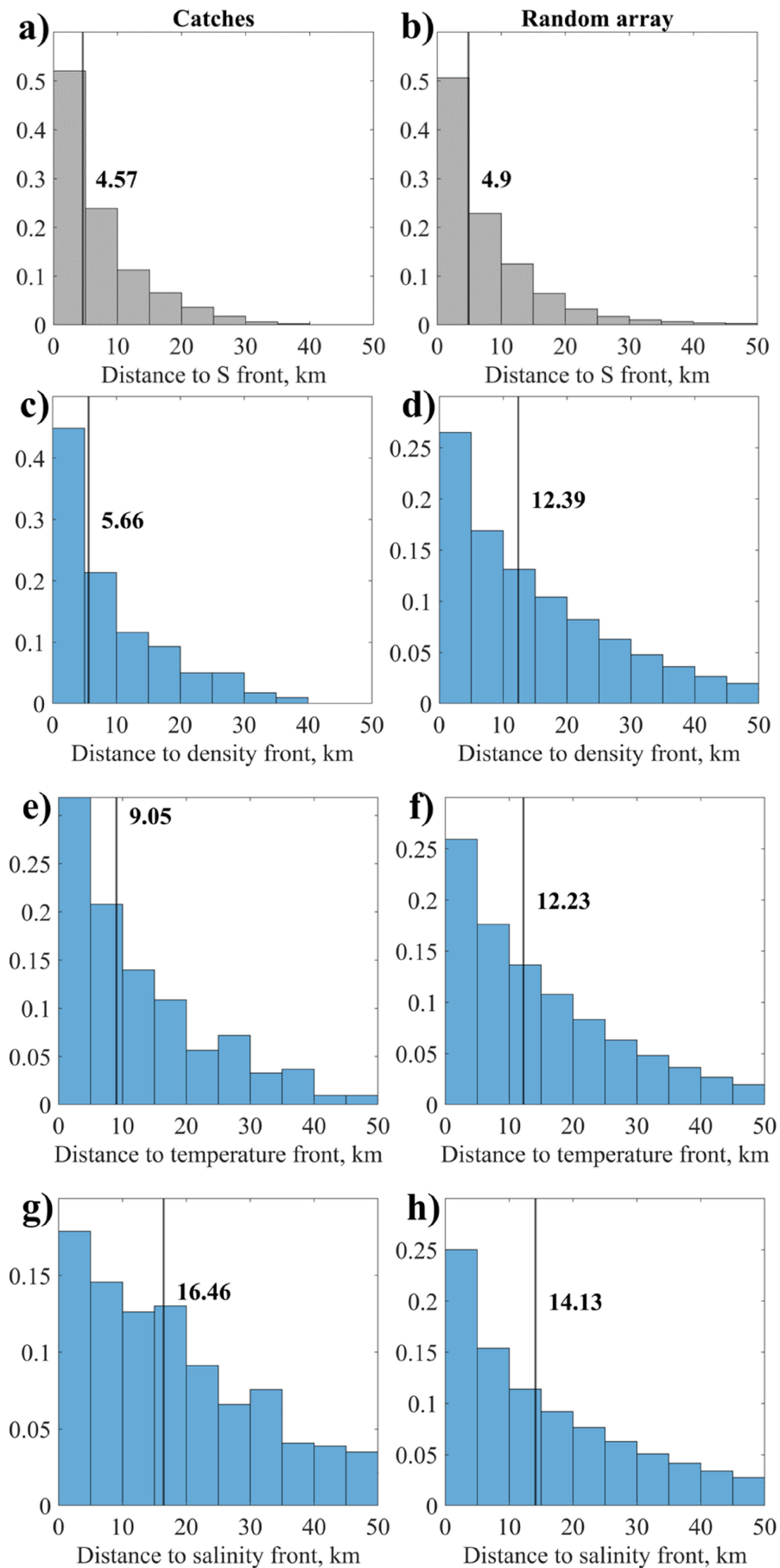
FIGURE 5 | Same as in Figure 4, with a distribution function threshold of 0.8.

References

Akhtyamova, A. F., and V. S. Travkin. 2023. "Investigation of Frontal Zones in the Norwegian Sea." *Physical Oceanography* 30, no. 1: 62–77. https://doi.org/10.29039/1573-160X-2023-1-62-77.

Belkin, I. M. 2002. "Front." In *Interdisciplinary Encyclopedia of Marine Sciences*, vol. 1: A–F, 433–435. Grolier Academic Reference.

Belkin, I. M. 2021. "Remote Sensing of Ocean Fronts in Marine Ecology and Fisheries." *Remote Sensing* 13, no. 5: 883. https://doi.org/10.3390/rs13050883.

Belkin, I. M., and P. C. Cornillon. 2007. "Fronts in the World Ocean's Large Marine Ecosystems." International Council for the Exploration of the Sea, 33 p. (ICES CM 2007/D:21).

Belonenko, T. V., V. S. Travkin, A. V. Koldunov, and D. L. Volkov. 2021. "Topographic Experiments Over Dynamical Processes in the Norwegian Sea." *Russian Journal of Earth Sciences* 21, no. 1: 1–15. https://doi.org/10.2205/2020ES000747.

Budyansky, M. B., S. V. Prants, E. V. Samko, and M. Y. Uleysky. 2017. "Identification and Lagrangian Analysis of Oceanographic Structures Favorable for Fishery of Neon Flying Squid (*Ommastrephes bartramii*) in the South Kuril Area." *Oceanology* 57, no. 5: 648–660. https://doi.org/10.1134/S0001437017050034.

Chuksin, Y. V., A. N. Provotorov, L. V. Simchenko, et al. 1977. "Size-Age Structure and Seasonal Changes in the Biological Condition of Mackerel in the Northeastern Atlantic." *Proceedings of VNIRO [Trudy VNIRO]* 121: 25–39 (In Russian).

Commercial Fish of Russia [Promyslovye ryby Rossii]. 2006. *In Two Volumes*, edited by O. F. Gritsenko, A. N. Kotlyar, and B. N. Kotenev, 1280. VNIRO Publishing (In Russian).

Fayman, P. A., S. V. Prants, M. V. Budyansky, and M. Y. Uleysky. 2019. "Coastal Summer Eddies in the Peter the Great Bay of the Japan Sea: In Situ Data, Numerical Modeling and Lagrangian Analysis." *Continental Shelf Research* 181: 143–155. https://doi.org/10.1016/j.csr.2019.05.002.

Fedorov, K. N. 1983. *Physical Nature and Structure of Oceanic Fronts*, 296. Gidrometeoizdat (In Russian).

Foux, V. R. 2009. "On Estimation of an Ocean Front Location Depending on the Satellite Measurements." *Fundamental and Applied Hydrophysics* 1, no. 1: 29–34 (In Russ.).

Gruzinov, V. M. 1986. *Hydrology of Frontal Zones of the World Ocean*, 272. Gidrometeoizdat (In Russian).

Johannessen, O. M. 1986. In *Brief Overview of the Physical Oceanography, the Nordic Seas*, edited by B. G. Hurdle, 103–128. Springer. https://doi.org/10.1007/978-1-4615-8035-5.

Kostianoy, A. G., and C. J. Nihoul. 2009. "Frontal Zones in the Norwegian, Greenland, Barents and Bering Seas." In *Influence of Climate Change on the Changing Arctic and Sub-Arctic Conditions*, 171–190. Springer. https://doi.org/10.1007/978-1-4020-9460-6_13.

Kostianoy, A. G., J. C. J. Nihoul, and V. B. Rodionov. 2004. *Physical Oceanography of Frontal Zones in the Subarctic Seas*. Vol. 71, 316 pp. (Elsevier Oceanography Series. Elsevier.

Malinin, V. N., and S. M. Gordeeva. 2009. "Fisheries Oceanography of the Southeastern Pacific." St. Petersburg: RSHU, Volume I: Variability of Habitat Factors, 277 pp. (In Russian).

Novoselova, E. V., P. A. Fayman, A. A. Didov, et al. 2024. "Modeling the Ventilation of the Vortex Periphery for Anticyclonic Quasi-Permanent Lofoten Vortex." *Pure and Applied Geophysics* 181: 3409–3429. https://doi.org/10.1007/s00024-024-03611-z.

Novoselova, E. V., V. S. Travkin, M. A. Lebedeva, A. A. Udalov, M. V. Budyansky, and T. V. Belonenko. 2024. "Features of the Vortex Structures in the Fields of Eulerian and Lagrangian Hydrological Characteristics for the Northwest Pacific." Vestnik of Saint Petersburg University. *Earth Sciences* 69, no. 2: 372–388. https://doi.org/10.21638/spbu07.2024.209 (In Russian).

Olden, J. D., and B. D. Neff. 2001. "Cross-Correlation Bias in Lag Analysis of Aquatic Time Series." *Marine Biology* 138: 1063–1070. https://doi.org/10.1007/s002270000517.

Owen, R. W. 1981. "Front and Eddies in the Sea: Mechanisms, Interaction and Biological Effects." In *Analysis of Marine Ecosystems*, 197–233. Academic press.

Prants, S. V. 2024. "Fisheries at Lagrangian Fronts." *Fisheries Research* 279: 107125. https://doi.org/10.1016/j.fishres.2024.107125.

Prants, S. V., M. V. Budyansky, and M. Y. Uleysky. 2014. "Identifying Lagrangian Fronts With Favourable Fishery Conditions." *Deep Sea Research Part I: Oceanographic Research Papers* 90: 27–35. https://doi.org/10.1016/j.dsr.2014.04.012.

Prants, S. V., M. V. Budyansky, M. Y. Uleysky, and V. V. Kulik. 2021. "Lagrangian Fronts and Saury Catch Locations in the Northwestern Pacific in 2004–2019." *Journal of Marine Systems* 222, no. L17203: 103605. https://doi.org/10.1016/j.jmarsys.2021.103605.

Prants, S. V., V. I. Ponomarev, M. V. Budyansky, M. Y. Uleysky, and P. A. Fayman. 2013. "Lagrangian Analysis of Mixing and Transport of Water Masses in the Marine Bays." *Izvestiya, Atmospheric and Oceanic Physics* 49, no. 1: 82–96. https://doi.org/10.1134/S0001433813010088.

Prants, S. V., V. I. Ponomarev, M. V. Budyansky, M. Y. Uleysky, and P. A. Fayman. 2015. "Lagrangian Analysis of the Vertical Structure of Eddies Simulated in the Japan Basin of the Japan/East Sea." *Ocean Modelling* 86: 128–140. https://doi.org/10.1016/j.ocemod.2014.12.010.

Smart, J. H. 1984. "Spatial Variability of Major Frontal Systems in the North Atlantic-Norwegian Sea Area: 1980–81." *Journal of Physical Oceanography* 14, no. 1: 185–192. https://doi.org/10.1175/1520-0485(1984)014<0185:SVOMFS>2.0.CO;2.

Vinogradov, M. E., A. A. Elizarov, and P. A. Moiseev. 1984. "Biological Productivity of Dynamically Active Zones in the Open Ocean." *Ocean Research*: 107–127 (In Russian).

Volkov, D. L., T. V. Belonenko, and V. R. Foux. 2013. "Puzzling Over the Dynamics of the Lofoten Basin—A Sub-Arctic Hot Spot of Ocean Variability." *Geophysical Research Letters* 40, no. 4: 738–743. https://doi.org/10.1002/grl.50126.

Volkov, D. L., A. Kubryakov, and R. Lumpkin. 2015. "Formation and Variability of the Lofoten Basin Vortex in a High-Resolution Ocean Model." *Deep-Sea Research Part I* 105: 142–157. https://doi.org/10.1016/j.dsr.2015.09.001.

Yu, L.-S., A. Bosse, I. Fer, et al. 2017. "The Lofoten Basin Eddy: Three Years of Evolution as Observed by Seagliders." *Journal of Geophysical Research, Oceans* 122, no. 8: 6814–6834. https://doi.org/10.1002/2017JC012982.